Polish Journal of Veterinary Sciences Vol. 17, No. 3 (2014), 413–420

DOI 10.2478/pjvs-2014-0059

Original article

Cytomorphometry of canine cutaneous histiocytoma

K. Paździor-Czapula, I. Otrocka-Domagała, T. Rotkiewicz, M. Gesek

Department of Pathological Anatomy, Faculty of Veterinary Medicine,
University of Warmia and Mazury in Olsztyn, Oczapowskiego 13, 10-719 Olsztyn, Poland

Abstract

A morphometric analysis of tumoral Langerhans cells and activated macrophages was conducted using canine cutaneous tumors (65 cases of canine cutaneous histiocytoma and 7 cases of pyogranuloma). The histiocytic origin of the tumor cells was confirmed using immunohistochemistry. The parameters of the morphometric analysis included cellular and nuclear size and shape and the nuclear:cytoplasmic ratio; the variability of these features was calculated separately for each tumor. The canine cutaneous histiocytoma group was divided into four stages of regression depending on the intensity of the lymphocytic infiltration. Statistical analysis revealed that the anisocytosis, anisokaryosis and cellular pleomorphism of tumoral Langerhans cells increased, while the cellular circularity and nuclear:cytoplasmic ratio decreased with tumor regression. Activated macrophages of the pyogranuloma were significantly larger, and had larger nuclei, than tumoral Langerhans cells. Furthermore, these activated macrophages showed greater anisocytosis and anisokaryosis and a lower nuclear:cytoplasmic ratio than tumoral Langerhans cells in the first stages of tumor regression. These results indicate that tumoral Langerhans cells undergo morphologic changes during the regression of canine cutaneous histiocytoma, reflecting their maturation and differentiation. Morphometry can be a useful method for distinguishing activated macrophages from tumoral Langerhans cells.

Key words: pyogranuloma, regression, Langerhans cell, histiocyte, macrophage, maturation, differentiation

Introduction

Canine cutaneous histiocytoma (CCH) is a fast growing tumor that occurs mostly in young dogs (Coomer and Liptak 2008). CCH is derived from epidermal dendritic cells (Langerhans cells) and undergoes spontaneous regression within 2-3 months (Moore et al. 1996, Schwens et al. 2011). The intensity of the lymphocytic infiltration is correlated with the degree of tumor regression and is characterized by focal coagulation necrosis and other degenerative changes of tumor cells (Cockerell and Slauson 1979). Tumor regression is connected with specific changes in tumor cells, such as transport of MHCII molecules from cytoplasmic vacuoles to the cell surface and loss of E-cadherin expression (Kipar et al. 1998, Pires et al. 2009). The nuclear area of CCH cells has a tendency to increase with tumor regression (Ciobotaru et al. 2004); however, other possible alterations of the morphology of tumoral Langerhans cells during regression have not yet been investigated.

Correspondence to: K. Paździor-Czapula, katarzyna.pazdzior@uwm.edu.pl, tel./fax: +48 89 523 34 58

Table 1. Primary antibodies, antigen retrieval and visualization systems.

Primary antibody	Clone	Dilution	Antigen retrieval	Visualization system
HLA-DR α chain (MHCII)[a]	monoclonal mouse anti-human TAL.1B5	1:20	2x3 min.[b] citrate buffer pH=6	EnVision+ System-HRP, Mouse (DAB)[a]
CD18[c]	monoclonal mouse anti-canine CA16.3C10	1:10	5 min. proteinase K[a]	EnVision+ System-HRP, Mouse (DAB)[a]
CD3[a]	polyclonal rabbit anti-human	1:50	2x3 min.[b] Tris-EDTA buffer pH=9	Impress Universal Reagent Anti-Mouse/ Rabbit Ig Peroxidase[d]
CD79αcy[a]	monoclonal mouse anti-human HM57	1:25	4x3 min.[b] Tris-EDTA buffer pH=9	EnVision+ System-HRP, Mouse (DAB)[a]
E-cadherin[a]	monoclonal mouse anti-human NCH-38	1:50	2x3 min.[b] Tris-EDTA buffer pH=9	EnVision+ System-HRP, Mouse (DAB)[a]

[a] Dako, Glostrup, Denmark
[b] Antigen retrieval was conducted in a microwave oven, 650W
[c] PF. Moore, Davis, CA
[d] Vector Laboratories Inc., Burlingame, CA

Morphometry, an auxiliary method in histopathology, is useful for detecting inconspicuous cellular and nuclear features that are easy to overlook in routine histopathological examination. This method provides reliable, objective and reproducible results (Smitha et al. 2011). Morphometric analysis was found to be useful in distinguishing benign from malignant canine mammary tumors (Simenov and Simenova 2006), and in the grading of canine cutaneous mast cell tumors (Strefezzi et al. 2003).

The diagnosis of CCH is often challenging, as different round cell tumors may have a similar morphology. Additional stains, including toluidine blue and immunohistochemistry (MHCII, CD18, CD3, CD79a) are most useful for the differentiation of canine cutaneous round cell tumors (Fernandez et al. 2005). Nuclear morphometry has been shown to be an effective auxiliary tool for differential diagnosis of histiocytoma, mastocytoma and transmissible venereal tumor in dogs (De Andrade Waldemarin et al. 2004). CCH (particularly the later regression stages) must also be distinguished from nodular granulomatous dermatitis, as both tumors are pleocellular with a prominent histiocytic component (Lee Gross et al. 2005, Schwens et al. 2011). Both histiocytic populations, macrophages and Langerhans cells, are derived from a common precursor from the bone marrow (Lee Gross et al. 2005). Phagocytic dermal macrophages undergo phenotypic transformation to Langerhans cells during immunologic reconstitution in humans (Murphy et al. 1986). The comparison of morphometrically measured cytological features of histiocytic cells, such as size, shape and variability (anisocytosis, anisokaryosis, cellular and nuclear pleomorphism), will be helpful in doubtful diagnostic cases, especially when the sample contains only a small number of cells.

The first aim of this study was to determine the influence of tumor regression on the morphology of tumoral cells of CCH, and the second aim was to compare the morphology of tumoral Langerhans cells of CCH in late stages of regression and activated macrophages of the pyogranuloma.

Materials and Methods

Solitary cutaneous tumors were collected from 72 dogs by surgical excisional biopsy. All tissue samples were immediately fixed in 10% buffered formalin, embedded in paraffin, cut into 3 μm sections and mounted on silanized glass. The sections were processed routinely and stained with hematoxylin and eosin. The tumors included 65 canine cutaneous histiocytomas (CCHs) and 7 pyogranulomas. The tumors were diagnosed on the basis of histopathological examination according to widely used criteria (Lee Gross et al. 2005). The immunohistochemical examination of each tumor was performed using an antibody panel (Table 1) and a visualization system based on the immunoperoxidase method with 3,3-diaminobenzidine (DAB) as a substrate. For every CCH, the intensity of the lymphocytic infiltration was evaluated on the 1-4 point scale (1=minimal; 2=moderate; 3=marked; 4=massive) of Cockerel & Slauson (1979).

Table 2. Methods of evaluation of morphometric parameters.

Morphometric parameter	Method/software	Unit
Cellular/nuclear perimeter	Tracing the outline (Panoramic Viewer)	μm
Cellular/nuclear area	Tracing the outline (Panoramic Viewer)	μm^2
Cellular/nuclear circularity	4πarea/perimeter^2 (Microsoft Excel)	–
Nuclear: cytoplasmic ratio	N area/(C area – N area) (Microsoft Excel)	–
Variability of parameter	Standard deviation/mean (Microsoft Excel)	–

Table 3. Pyogranuloma morphometry summary data: number of cases (n), minimal and maximal values of evaluated parameters and mean value with standard deviation (SD).

Morphometric parameters	N	Min.	Max.	Mean	SD
Cellular area (μm^2)	7	73.12	160.76	110.33	26.896
Variability of cellular area	7	0.20	0.37	0.29	0.059
Cellular perimeter (μm)	7	32.48	48.25	39.65	4.855
Variability of cellular perimeter	7	0.11	0.19	0.15	0.028
Cellular circularity	7	0.82	0.89	0.86	0.022
Variability of cellular circularity	7	0.06	0.10	0.08	0.016
Nuclear area (μm^2)	7	27.26	36.08	32.47	2.757
Variability of nuclear area	7	0.23	0.39	0.31	0.058
Nuclear perimeter (μm)	7	20.48	23.53	22.09	1.101
Variability of nuclear perimeter	7	0.11	0.20	0.16	0.034
Nuclear circularity	7	0.74	0.87	0.82	0.042
Variability of nuclear circularity	7	0.07	0.14	0.10	0.022
N:C ratio	7	0.28	0.67	0.50	0.141
Variability of N:C ratio	7	0.30	0.72	0.44	0.139

Morphometric analysis was conducted using slides stained with hematoxylin and eosin. Histiocytic cells were evaluated in five randomly chosen areas (400x magnification) of the slide, including approximately 10 cells/area (50 cells/tumor) and avoiding necrotic foci. The parameters of the morphometric analysis included cellular and nuclear size (perimeter and area), which were measured by tracing the outline of the cell and the nucleus and calculated automatically using Panoramic Viewer software (3DHISTECH, Hungary) (Table 2). For each tumor, approximately 100 measurements were performed (yielding a total of 7200 measurements for the complete study). For each cell, the cellular and nuclear circularity was determined (circularity = 4πarea/perimeter^2) in addition to the nuclear:cytoplasmic ratio (N:C ratio; N:C = N area/(C area – N area)) (Smitha et al., 2011) (Table 2).

Microscopic evaluation of the slides was conducted using a MIDI Panoramic Scanner (3DHISTECH, Hungary) and Panoramic Viewer software. All the measurements were analyzed using Microsoft Excel (2010) software. The results are expressed as means together with standard deviations. Further mathematical analysis included the variability (coefficient of variation) of every evaluated parameter (Table 2).

The scores of the two groups were compared using Student's t test for symmetrical data and the Mann-Whitney U test for asymmetrical data. Spearman rank correlation analysis was used to detect correlations between the intensity of the lymphocytic infiltration and the morphometric parameters of tumoral Langerhans cells (r: Spearman rank correlation coefficient). The differences or correlations were considered statistically significant when $P< 0.05$. Statistical analysis was performed using Statistica software (Statsoft 10 eng. 32 bit).

Results

The histiocytic origin of tumoral Langerhans cells and activated macrophages of pyogranuloma was confirmed by immunohistochemical examination

Table 4. CCH morphometry summary data: number of cases (n), minimal and maximal values of evaluated parameters and mean value with standard deviation (SD).

Morphometric parameters	N	Min.	Max.	Mean	SD
Cellular area (μm^2)	65	40.80	118.99	79.08	18.245
Variability of cellular area	65	0.15	0.46	0.24	0.055
Cellular perimeter (μm)	65	24.91	42.50	33.74	4.072
Variability of cellular perimeter	65	0.08	0.23	0.12	0.026
Cellular circularity	65	0.77	0.89	0.85	0.025
Variability of cellular circularity	65	0.04	0.11	0.07	0.015
Nuclear area (μm^2)	65	17.24	42.32	27.76	5.308
Variability of nuclear area	65	0.16	0.39	0.27	0.048
Nuclear perimeter (μm)	65	16.34	25.06	20.23	1.845
Variability of nuclear perimeter	65	0.08	0.20	0.14	0.027
Nuclear circularity	65	0.74	0.88	0.83	0.027
Variability of nuclear circularity	65	0.06	0.16	0.09	0.020
N:C ratio	65	0.42	1.07	0.61	0.138
Variability of N:C ratio	65	0.23	0.56	0.38	0.061

(MHCII+, CD18+, CD79-, CD3-) in each case. Additionally, the tumoral Langerhans cells expressed E-cadherin, while activated macrophages of pyogranuloma were consistently E-cadherin negative.

The results of the morphometric analysis are presented in Table 3 (pyogranuloma) and Table 4 (CCH). Lymphocytic infiltration was minimal in 13 CCHs (20%), moderate in 27 CCHs (42%), marked in 17 CCHs (26%) and massive in 8 CCHs (12%). The intensity of lymphocytic infiltration was positively correlated with the variability of the cellular perimeter (r=0.406; P=0.001) and the variability of the cellular area (r=0.353; P=0.004) as well as with the variability of the nuclear perimeter (r=0.364; P=0.003) and the variability of the nuclear area (r=0.340; P=0.006) of tumor cells. The intensity of lymphocytic infiltration was negatively correlated with the cellular circularity (r=-0.301; P=0.015) and the N:C ratio (r=-0.478; P=0.000) of tumor cells. The variability of the cellular circularity (r=0.259; P=0.037) and the variability of the N:C ratio (r=0.259; P=0.038) of tumor cells were positively correlated with the intensity of lymphocytic infiltration.

Statistical analysis revealed that the cellular perimeter (P=0.001) and area (P=0.000) as well as the nuclear perimeter (P=0.025) and area (P=0.000) differed significantly between the pyogranuloma and CCH with minimal to moderate lymphocytic infiltration groups. The cellular perimeter (P=0.007) and area (P=0.005) as well as the nuclear perimeter (P=0.006) and area (P=0.012) differed significantly also between the pyogranuloma and CCH with marked to massive lymphocytic infiltration groups. The activated macrophages of the pyogranuloma were larger, and had larger nuclei, than the tumoral Langerhans cells (Fig. 1, 2). The variability of the cellular perimeter (P=0.003), variability of the cellular area (P=0.001), variability of the nuclear perimeter (P=0.003), variability of the nuclear area (P=0.007) and the N:C ratio (P=0.042) differed significantly between the pyogranuloma and CCH with minimal to moderate lymphocytic infiltration groups. The activated macrophages of the pyogranuloma showed greater anisocytosis and anisokaryosis and a lower N:C ratio than the tumoral Langerhans cells from CCH with minimal to moderate lymphocytic infiltration (Fig. 3). These parameters did not differ significantly between the pyogranuloma and CCH with marked to massive lymphocytic infiltration groups (Fig. 4).

Discussion

Lymphocyte-dependent CCH regression is connected with the maturation of tumor cells. The different maturation states of the tumoral cells during CCH regression reflect the natural life cycle of normal Langerhans cells (Baines et al. 2000, Pires et al. 2009). During the regression process, immunophenotypical

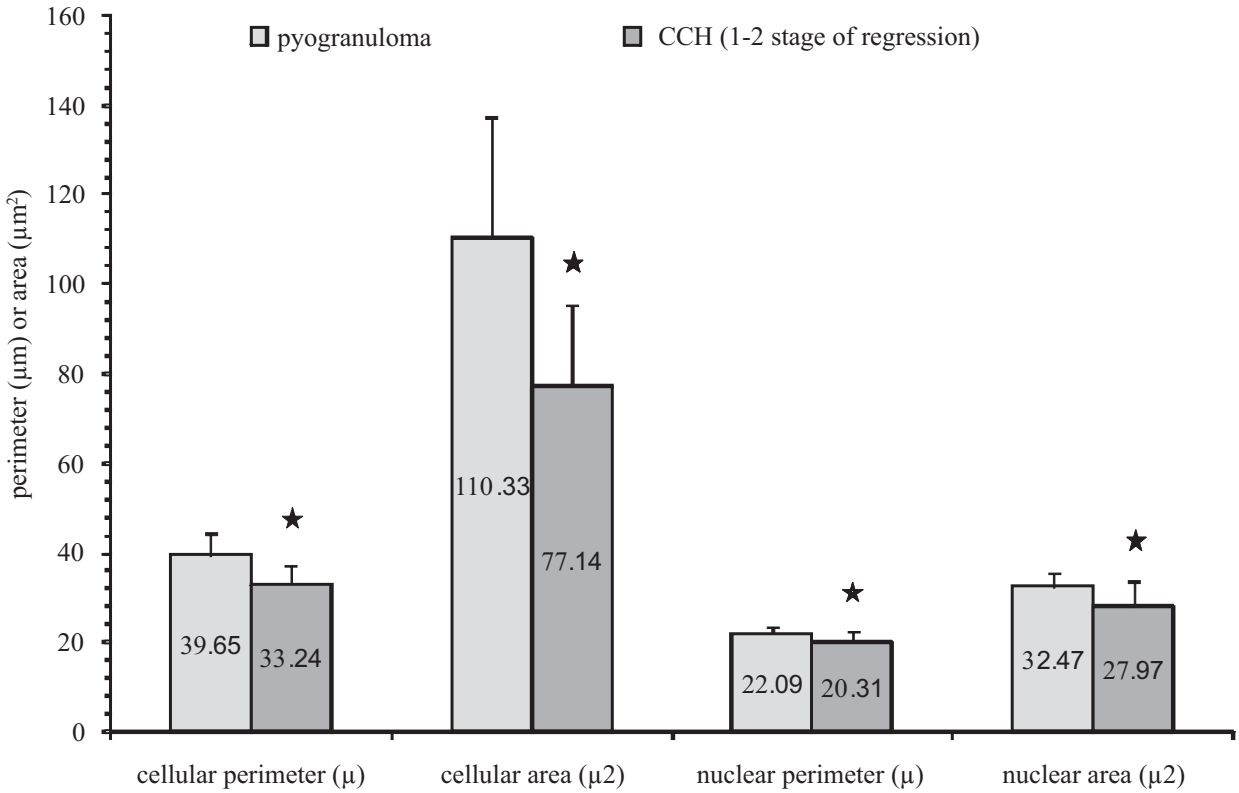

Fig. 1. Cellular and nuclear size of activated macrophages of pyogranuloma and tumoral Langerhans cells of CCH with minimal to moderate lymphocytic infiltration (1-2 stage of regression). The arithmetic mean of cellular perimeter, cellular area, nuclear perimeter and nuclear area is placed in the middle of each column. Statistically significant differences are marked with an asterisk.

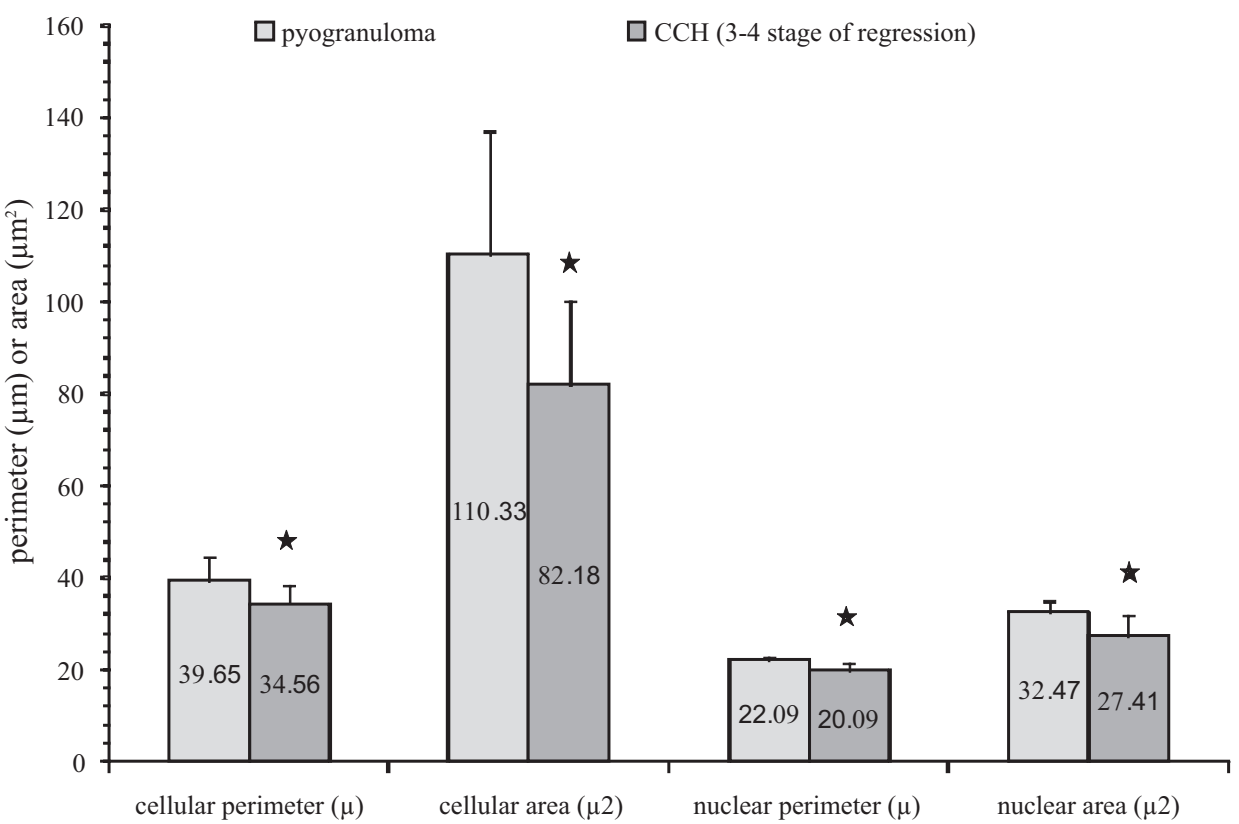

Fig. 2. Cellular and nuclear size of activated macrophages of pyogranuloma and tumoral Langerhans cells of CCH with marked to massive lymphocytic infiltration (3-4 stage of regression). The arithmetic mean of cellular perimeter, cellular area, nuclear perimeter and nuclear area is placed in the middle of each column. Statistically significant differences are marked with an asterisk.

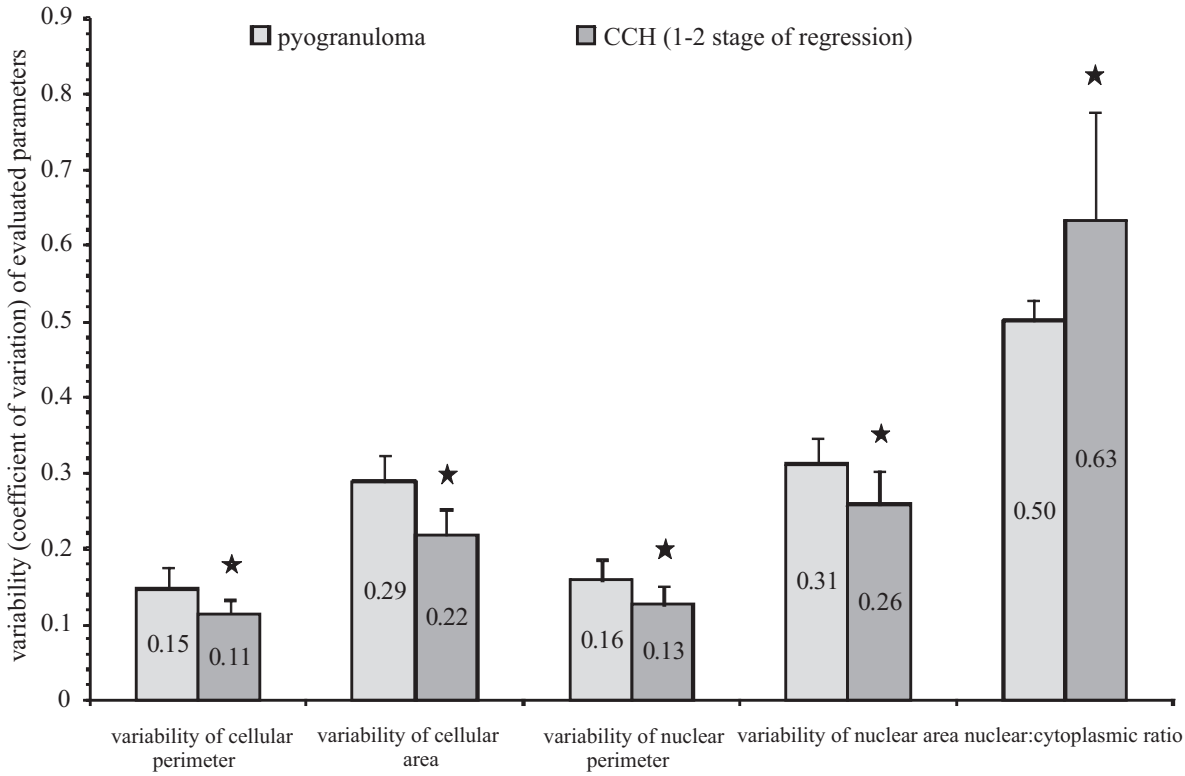

Fig. 3. Anisocytosis (variability of the cellular perimeter and area), anisokaryosis (variability of the nuclear perimeter and area) and N:C ratio of activated macrophages (pyogranuloma) and tumoral Langerhans cells of CCH with minimal to moderate lymphocytic infiltration (1-2 stage of regression). The arithmetic mean of variability of cellular perimeter, variability of cellular area, variability of nuclear perimeter, variability of nuclear area and nuclear: cytoplasmic ratio is placed in the middle of each column. Statistically significant differences are marked with an asterisk.

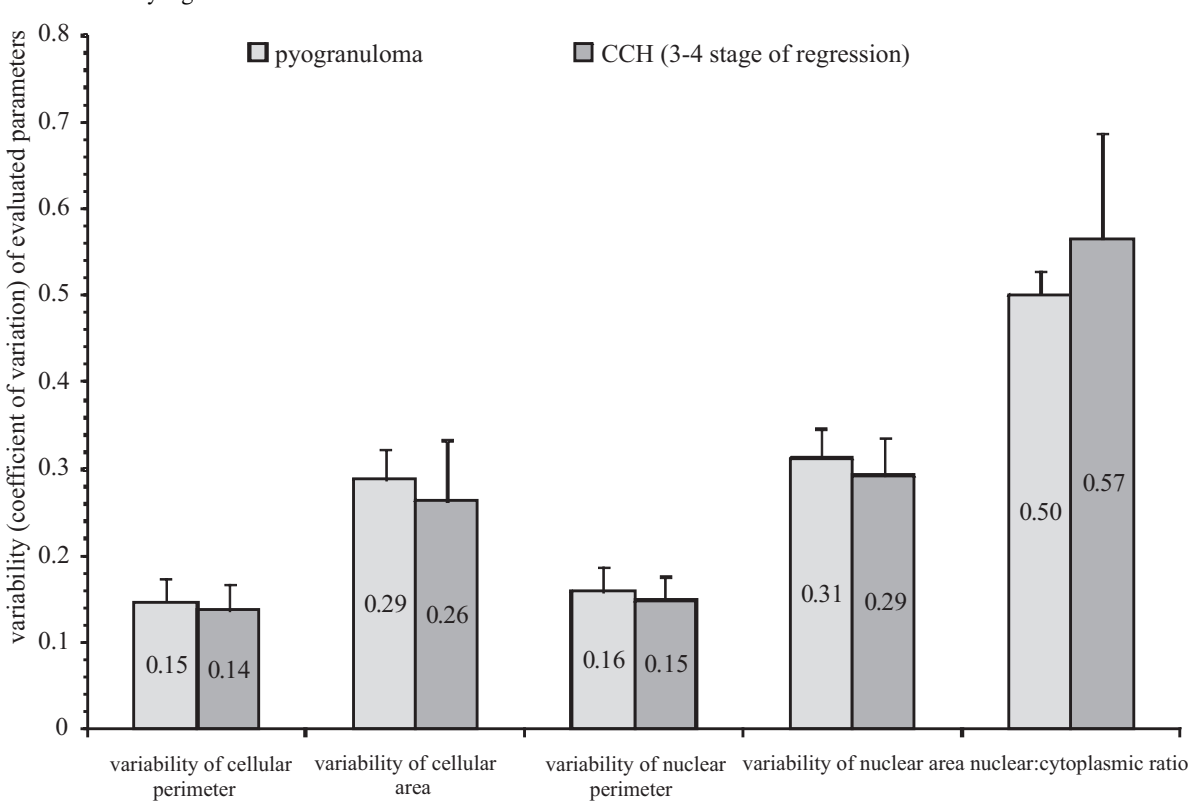

Fig. 4. Anisocytosis (variability of cellular perimeter and area), anisokaryosis (variability of nuclear perimeter and area) and N:C ratio of activated macrophages (pyogranuloma) and tumoral Langerhans cells of CCH with marked to massive lymphocytic infiltration (3-4 stage of regression). The arithmetic mean of variability of cellular perimeter, variability of cellular area, variability of nuclear perimeter, variability of nuclear area and nuclear:cytoplasmic ratio is placed in the middle of each column.

changes occur in tumor cells. Similar to the normal Langerhans cells, which lose E-cadherin expression when they migrate from the epidermis to the local lymph nodes, the E-cadherin expression in CCH decreases with the regression stage (Piers et al. 2009). The maturation of normal Langerhans cells is connected with redistribution of MHCII from intracellular compartments to the cell surface (Mellman and Steinman 2001). The spontaneous regression of CCH develops as a consequence of the transport of MHCII from cytoplasmic vesicles to the cell membrane of tumor cells (Kipar et al. 1998, Pires et al. 2013). The results of this study revealed that tumor regression is accompanied by changes in the cellular and nuclear morphology of tumor cells. The degree of anisocytosis and anisokaryosis as well as the cellular pleomorphism of tumoral Langerhans cells increased with tumor regression, as demonstrated by the positive correlations between the intensity of lymphocytic infiltration and the variability in cellular size, cellular shape, nuclear size and the N:C ratio. Furthermore, the circularity of tumoral Langerhans cells decreased with the degree of tumor regression. We suggest that the increase in anisocytosis, anisokaryosis and cellular pleomorphism of tumor cells in CCH with the regression stage probably reflects the maturation of tumor cells. Ciobotaru et al. (2004) revealed that the nuclear area of tumoral Langerhans cells in the second and third stage of the regression is larger than that in the first stage of this process. The present study revealed the decrease in the N:C ratio with the intensity of lymphocytic infiltration. The N:C ratio is an indicator of cellular differentiation. Well-differentiated cells usually have a lower N:C ratio than their poorly differentiated counterparts (McGavin and Zachary 2012). The results of this study suggest that CCH cells achieve a higher degree of differentiation during regression. It is possible that normal Langerhans cells undergo morphological changes during maturation that are similar to those of CCH cells during regression.

Dendritic cells, including Langerhans cells, can be distinguished from macrophages by their poor phagocytic activity and paucity of intracellular organelles (Wright-Browne et al. 1997). Macrophages are characterized by pronounced phagocytic activity, although some dendritic cells also have phagolysosomes which consume dead nucleated cells (Wright-Browne et al. 1997, Lee Gross et al. 2005). The results of this study revealed that the activated macrophages of pyogranuloma were larger and had larger nuclei than the tumoral Langerhans cells, in both early and late stages of regression. Therefore, cellular and nuclear sizes are features that can be used to differentiate activated macrophages from tumoral Langerhans cells. We suggest that the cellular and nuclear size could also be useful in differentiation between reactive proliferation of dendritic cells (reactive histiocytosis) and nodular pyogranulomatous inflammation; however, further research is needed to verify this hypothesis. The current study indicates that activated macrophages show greater anisocytosis and anisokaryosis as well as a lower N:C ratio than tumoral Langerhans cells in tumors in the early stages of regression. These features did not differ significantly between activated macrophages and tumoral Langerhans cells in the late stages of CCH regression. These results suggest that marked anisocytosis and anisokaryosis is a feature of differentiated histiocytic cells. Although reactive cell populations are believed to be generally more homogenous than their neoplastic counterparts, both reactive and neoplastic macrophages can show similar anisocytosis and anisokaryosis (Weiss 2001, McGavin and Zachary 2012).

In conclusion, tumoral Langerhans cells undergo specific morphological changes during regression of CCH, which most likely reflects their maturation and differentiation. Morphometry can be a useful method for differentiating activated macrophages from tumoral Langerhans cells of CCH in late stages of regression.

References

Baines SJ, Bujdoso R, Backlaws BA, McInnes E, Moore PF, McConnel IM (**2000**) Maturation states of dendritic cells in canine cutaneous histiocytoma. Vet Dermatol 11 (Suppl 1): 9-10.

Ciobotaru E, Militaru M, Soare T, Mocanu J, Bartoiu A (**2004**) Canine cutaneous histiocytoma: morphology and morphometry. Vet Dermatol 15 (Suppl 1): 62.

Cockerell GL, Slauson DO (**1979**) Patterns of lymphoid infiltrate in the canine cutaneous histiocytoma. J Comp Pathol 89: 193-203.

Coomer AR, Liptak JM (**2008**) Canine histiocytic diseases. Compend Contin Educ Vet 30: 202-216.

De Andrade Waldemarin KC, Beletti ME, Da Fontoura Costa L (**2004**) Nuclear morphometry of neoplastic cells as a method for diagnosis of histiocytoma, mastocytoma and transmissible venereal tumor in dogs. Real-Time Imaging 10: 197-204.

Fernandez NJ, West KH, Jackson ML, Kidney BA (**2005**) Immunohistochemical and histochemical stains for differentiating canine cutaneous round cell tumors. Vet Pathol 42: 437-445.

Kipar A, Baumgärtner W, Kremmer E, Frese K, Weiss E (**1998**) Expression of major histocompatibility complex class II antigen in neoplastic cells of canine cutaneous histiocytoma. Vet Immunol Immunopathol 62: 1-13.

Lee Gross T, Ihrke PJ, Walder WJ, Affolter VK (**2005**) Skin diseases of the dog and cat. Clinical and histopathologic diagnosis, 2nd ed., Blackwell Science Ltd, Oxford.

McGavin MD, Zachary JF (**2012**) Pathologic basis of veterinary disease, 5th ed., Mosby Elsevier, St Louis.

Mellman I, Steinman RM (**2001**) Dendritic cells: specialized and regulated antigen processing machines. Cell 106: 255-258.

Moore PF, Schrenzel MD, Affolter VK, Olivry T, Naydan D (**1996**) Canine cutaneous histiocytoma is an epidermotropic Langerhans cell histiocytosis that expresses CD1 and specific beta 2-integrin molecules. Am J Pathol 148: 1699-1708.

Murphy GF, Messadi D, Fonferko E, Hancock WW (**1986**) Phenotypic transformation of macrophages to Langerhans cells in the skin. Am J Pathol 123: 401-406.

Pires I, Queiroga FL, Alves A, Silva F, Lopes C (**2009**) Decrease of E-cadherin expression in canine cutaneous histiocytoma appears to be related to its spontaneous regression. Anticancer Res 29: 2713-2717.

Pires I, Rodriques P, Alves A, Queiroga FL, Silva F, Lopes C (**2013**) Immunohistochemical and immunoelectron study of major histocompatibility complex class-II antigen in canine cutaneous histiocytoma: its relation to tumor regression. In Vivo 27: 257-262.

Schwens Ch, Thom N, Moritz A (**2011**) Reactive and neoplastic histiocytic diseases in the dog. Tierarztl Prax Ausg K Kleintiere Heimtiere 39: 176-190.

Simeonov R, Simeonova G (**2006**) Computerized morphometry of mean nuclear diameter and nuclear roundness in canine mammary gland tumors on cytologic smears. Vet Clin Pathol 35: 88-90.

Smitha T, Sharada P, Girish HC (**2011**) Morphometry of the basal cell layer of oral leukoplakia and oral squamous cell carcinoma using computer-aided image analysis. J Oral Maxillofac Pathol 15: 26-33.

Strefezzi R de F, Xavier JG, Catão-Dias JL (**2003**) Morphometry of canine cutaneous mast cell tumors. Vet Pathol 40: 268-275.

Weiss DJ (**2001**) Cytologic evaluation of benign and malignant hemophagocytic disorders in canine bone marrow. Vet Clin Pathol 30: 28-34.

Wright-Browne V, McClain KL, Talpaz M, Ordonez N, Estrov Z (**1997**) Physiology and pathophysology of dendritic cells. Hum Pathol 28: 563-579.